

Electronic four-particle correlations in semiconductors: Renormalization of coherent pump-probe oscillations

U. Neukirch,* S. R. Bolton,† L. J. Sham,‡ and D. S. Chemla

Department of Physics, University of California and Materials Sciences Division, Lawrence Berkeley National Laboratory,
1 Cyclotron Road, MS 2-346, Berkeley, California 94720

(Received 21 September 1999)

The nonlinear optical response of excitons in a single ZnSe quantum well is investigated by pump-probe measurements. In the counter-circular polarization configuration at negative delay, Δt , spectral oscillations are observed the period E_{PP} of which is energy dependent. Whereas at energies above the 1S exciton the usual $E_{PP} = h/|\Delta t|$ dependence is found, the period strongly deviates from that value at energies below the exciton. Model calculations reveal that this behavior is caused by the bound biexciton state in the four-particle correlations.

In 1987 it was shown that oscillatory structures appear in pump-probe (P&P) spectra of semiconductors at negative delay Δt , i.e., when the probe pulse arrives on the sample before the pump pulse.¹ This seemingly noncausal behavior is due to the nonlinear interaction of the pump field with the coherent macroscopic polarization still present from the preceding probe. The lowest-order nonlinear P&P contribution is due to four-photon (= third-order) processes which scatter pump photons into the probe direction \mathbf{k}_1 ($=\mathbf{k}_1 + \mathbf{k}_2 - \mathbf{k}_2$; with \mathbf{k}_1 and \mathbf{k}_2 being the respective wave vectors of the probe and the pump beam). The superposition of the first-order (= transmitted probe) and the delayed coaxial third-order contribution then leads to oscillations in the spectral domain the period of which was found to be $E_{PP} = h/|\Delta t|$.^{2,3} Note that within the usual four-wave mixing (FWM) nomenclature, the time sequence for *negative* pump-probe delay — \mathbf{k}_1 first, \mathbf{k}_2 second — corresponds to *positive* FWM delay. Because of their supposedly regular delay dependence, P&P oscillations have been used as an internal clock to evaluate propagation effects in P&P experiments with spatially displaced spots.⁴

Recently, it has been shown that electronic higher-order correlations — which involve at least four particles — have a profound effect on the FWM response of semiconductors.^{5–10} Furthermore, the analysis of data from a microcavity revealed that its P&P response in counter-circular polarization configuration is dominated by effects caused by the bound biexciton,¹¹ the latter being the most prominent consequence of correlation between four particles. In view of these results, the question naturally arises how the coherent P&P oscillations around a single exciton resonance are affected by four-particle correlations.

In this paper, the problem of coherent P&P oscillations is reexamined for a wide-band-gap ZnSe quantum well (QW) which exhibits a strong biexciton binding. It is shown that in the counter-circular polarization configuration, which allows for excitation of the bound biexciton state, the period of the oscillations is strongly altered in the spectral vicinity of the exciton-biexciton transition. Model calculations in which four-particle correlations are accounted for result in good agreement with the experimental data. Moreover, the coherent part of the response is shown to be qualitatively reproduced when the only nonlinearity in the model is that induced by the biexciton.

The sample was prepared by molecular beam epitaxy on a GaAs substrate and consists of a single 5 nm ZnSe quantum well (QW) embedded in $\text{Zn}_{1-x}\text{Mg}_x\text{S}_y\text{Se}_{1-y}$ barriers. For measurements in transmission geometry, the sample was glued on a sapphire disc, then the substrate was partially ground down, and subsequently completely removed by wet chemical etching. Measurements were performed at a sample temperature of 12 K using carefully dispersion-compensated 70 fs pulses from a frequency-doubled Ti:sapphire laser.

In Fig. 1, differential transmission spectra $\Delta T/T$ of the sample are shown in a contour plot for counter-circular polarization. At negative delay, the expected oscillatory structure appears. It is very pronounced at energies below the exciton but considerably weaker at energies above. For positive delay, the main effect — which extends well into the incoherent regime — is a bleaching and a slight blue shift of the exciton (at 2.825 eV). A line of induced absorption ap-

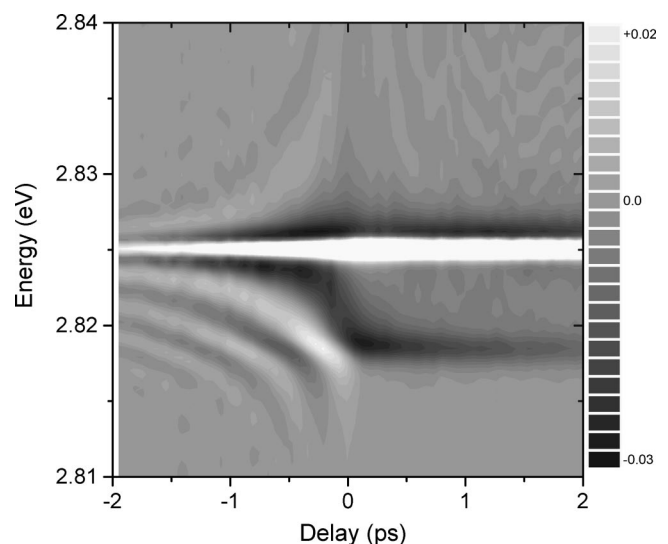


FIG. 1. Experimental spectrally resolved differential transmission $\Delta T(\omega)/T(\omega) := (T^* - T)/T$ of the sample in dependence on the delay Δt between pump and probe pulses. Here, T^* (T) denotes the transmission through the sample with the pump beam on (off). Polarizations of pump/probe/detection are $\sigma^-/\sigma^+/\sigma^+$. Note that the strong response right at the exciton line is positive and is off the scale. Its maximum reads +0.17.

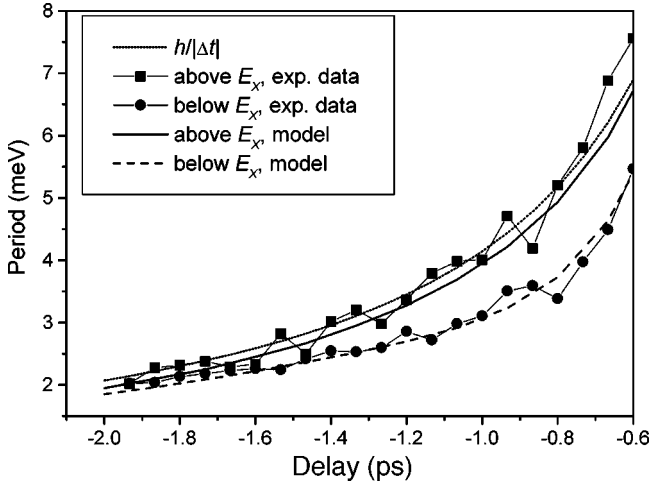


FIG. 2. Oscillation period E_{PP} at negative delay Δt as deduced from Fig. 1 at energies slightly above (squares) and below (dots) the 1S-hh exciton. The solid (dashed) line is the period above (below) the exciton as it results from model calculations. The dotted line is given by $E_{PP} = -h/|\Delta t|$.

pears around the exciton-biexciton transition energy (≈ 2.818 eV) for $\Delta t > 0$. From this excited-state absorption, a biexciton binding energy of 6.6 meV is deduced in agreement with a thorough FWM investigation on another piece of the same sample.⁹ This absorptive effect develops around zero delay smoothly out of the first minimum of the coherent oscillations below the exciton line. The asymmetry in visibility of the oscillations is accompanied by an asymmetry in their spectral period. This is shown in Fig. 2 where the oscillation periods above (squares) and below (dots) the exciton line are displayed versus the pump-probe delay. The oscillation periods shown in Fig. 2 were determined using an identical technique above and below the excitonic resonance. In each case, the period was obtained from an average of two sequential cycles of oscillation, starting with the cycle adjacent to the exciton resonance. Whereas the period found at energies above the exciton follows the $h/|\Delta t|$ dependence, around the exciton-biexciton transition energy the period is less than $h/|\Delta t|$ throughout the whole range of delays.

Because of the obvious biexcitonic contributions, a model of the above observations requires a theory which treats exciton-correlation effects beyond the Hartree-Fock approximation. We base our analysis on the ‘‘average polarization model’’¹² derived by averaging over the nonlinear excitonic contributions from the dynamics-controlled-truncation scheme¹³ developed for the coherent regime. Its coupled equations of motion involve only spin-dependent polarization variables, \mathcal{P} , and one four-particle correlation variable (or biexciton two-photon coherence) \mathcal{B} . The interaction parameters are not computed from first principles but are adjusted by hand. The model was formulated before in a version including the effects of a microcavity in which the same sample was placed.¹¹ This formulation allows also for a treatment of the bare sample where the outer boundaries of barrier layers act as mirrors with a correspondingly low reflectivity. The electric field inside the heterostructure \mathcal{E} is driven by the external field \mathcal{E}^{ext} through a coupling rate g .¹⁴ The coupling between the field \mathcal{E} and the QW polarization \mathcal{P} is described by κ in both their equations of motion. The

first-order fields and polarizations obey

$$\frac{\partial}{\partial t} \mathcal{E}_{p/t}^{(1)} = (i(\omega_C - \omega_0) - \Gamma_C) \mathcal{E}_{p/t}^{(1)} - i\kappa \mathcal{P}_{p/t}^{(1)} + g \mathcal{E}_{p/t}^{ext}, \quad (1)$$

$$\frac{\partial}{\partial t} \mathcal{P}_{p/t}^{(1)} = (i(\omega_X - \omega_0) - \Gamma_X) \mathcal{P}_{p/t}^{(1)} - i\kappa \mathcal{E}_{p/t}^{(1)}, \quad (2)$$

where p and t label the pump and probe (test) of frequency ω_0 , and ω_C , Γ_C , ω_X , and Γ_X are the frequencies and dephasing rates of the photon mode (inside the heterostructure) and the exciton. The third-order probe field is driven by the third-order polarization

$$\frac{\partial}{\partial t} \mathcal{E}_t^{(3)} = (i(\omega_C - \omega_0) - \Gamma_C) \mathcal{E}_t^{(3)} - i\kappa \mathcal{P}_t^{(3)}, \quad (3)$$

and the third-order polarization in the probe direction for co- and counter-polarized pump evolves according to

$$\frac{\partial}{\partial t} \mathcal{P}_{+t}^{(3)} = (i(\omega_X - \omega_0) - \Gamma_X) \mathcal{P}_{+t}^{(3)} - i\kappa \mathcal{E}_{+t}^{(3)} \quad (4)$$

$+i\kappa \mathcal{E}_{+t}^{(1)} \frac{ \mathcal{P}_{+p}^{(1)} ^2}{P_S^2}$		$+0$
$+i\kappa \mathcal{E}_{+p}^{(1)} \frac{\mathcal{P}_{+p}^{(1)*} \mathcal{P}_{+t}^{(1)}}{P_S^2}$		$+0$
$+i(\tilde{V} - V_s) \mathcal{P}_{+t}^{(1)} \mathcal{P}_{+p}^{(1)} ^2$		$-iV_s \mathcal{P}_{+t}^{(1)} \mathcal{P}_{-p}^{(1)} ^2$
$+0$		$+iV_B \mathcal{B} \mathcal{P}_{-p}^{(1)*}$

Here the indices $+$ and $-$ label the polarization states. For comparison, Eq. (4) is presented as a table with the nonlinear source terms active for co- and counter-polarized pump written, respectively, in the left and right column. The first two sources describe phase-space filling characterized by the saturation parameter P_S and contribute only for co-polarization. \tilde{V} includes the mean-field Coulomb interaction and the exciton exchange, and V_s the exciton screening.¹⁵ The last term characterized by V_B accounts for the biexciton-exciton interaction and contributes only for counter-polarization. Finally \mathcal{B} , which is only nonzero for counter-polarized beams, evolves according to:

$$\frac{\partial}{\partial t} \mathcal{B} = (i(\omega_{XX} - 2\omega_0) - \Gamma_{XX}) \mathcal{B} + i\mathcal{P}_{-p}^{(1)} \mathcal{P}_{+t}^{(1)} \quad (5)$$

Here, ω_{XX} and Γ_{XX} are the frequency and the dephasing of the biexciton. All terms in Eq. (4) are derived from a microscopic basis.^{15,16} The equations of motion are numerically integrated, with most parameters deduced from the experimental conditions ($\mathcal{E}^{ext}, \omega_0$), the linear transmission of the sample ($\omega_X, \Gamma_X, \kappa$), and from the P&P response at large delay (ω_{XX}). The value of the photon damping rate Γ_C is estimated from the respective reflectivity of the barrier-Helium and the barrier-glu interfaces. It turns out to be so large (> 60 meV) that the calculated result becomes insensitive to this quantity. With that, the resonance frequency of the photon mode within the heterostructure ω_C only affects the magnitude of the overall transmission but not its spectral

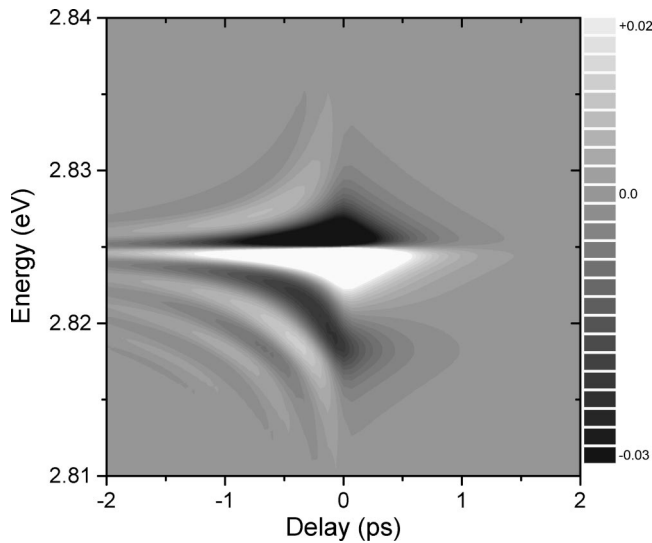


FIG. 3. Calculated spectrally resolved differential transmission $\Delta T/T$ in dependence on the delay Δt between pump and probe pulses. The only nonlinearity accounted for is the exciton-biexciton interaction V_B . Note that the strongest response right at the exciton line is off the scale.

shape. For simplicity, it is set being equal to the exciton energy ω_X . The biexciton damping Γ_{XX} was set to twice the exciton damping.

In counter-circular polarization the only nonlinear sources are exciton screening V_s and the exciton-biexciton interaction V_B . In Fig. 3, a set of P&P spectra is displayed calculated with V_B as the only nonlinearity. Obviously, this is already sufficient to describe qualitatively all features observed in the experiment for negative and around zero delay. Compared to energies above the exciton, the visibility of the coherent oscillations is strongly enhanced around the exciton-biexciton transition energy. The first minimum below the exciton evolves into the induced absorption line of exciton-biexciton transitions. Finally, the asymmetry of the period exactly corresponds to the experimental observation. This is shown in Fig. 2 where the solid (dashed) line shows

the period obtained from the calculated spectra above (below) the exciton energy. At positive delay the calculated response rapidly decreases since effects due to incoherent excitons are not included here (see above). To account for such effects like exciton-biexciton transitions in the incoherent regime requires the inclusion of six-particle correlations^{17,18} which is far beyond the scope of this paper.

Note that the rise time of the signal is larger than its decay time. This is opposite to the FWM response^{19,20} and is just due to the inverted definitions of the delay time axes for FWM and P&P experiments. Use of exciton screening V_s as the only nonlinear source yields a perfectly symmetric response around the exciton with similar visibility and a single oscillation period very close to $h/|\Delta t|$. Moreover, the phase of the coherent oscillations is then opposite to the one observed in the experiment. This sign inversion with respect to the response caused by the mean-field Coulomb interaction was recently also observed in the polarization dependence of the optical Stark effect.¹⁰ So, the inclusion of a dominant biexciton-induced nonlinearity is necessary to describe the experimental observations in agreement with findings on a ZnSe-based microcavity.¹¹

In summary, we have shown that the period of coherent pump-probe oscillations is renormalized to smaller values in the vicinity of the exciton-biexciton transition energy. The calculation of this effect needs to account for four-particle correlations beyond the Hartree-Fock approximation. Moreover, the coherent part of the nonlinear response is qualitatively well described by a model accounting only for the biexciton-induced correlation.

This work was supported by the Director, Office of Energy Research, Office of Basic Energy Sciences, Division of Material Sciences of the U.S. Department of Energy, under Contract No. DE-AC03-76SF00098. The authors would like to thank J. Nürnberger and W. Faschinger (Univ. Würzburg) for providing the ZnSe heterostructure, and N. Fromer for providing the program code for the calculations. One of us (U.N.) would like to thank the Max-Kade Foundation for funding.

*Present address: Institut für Festkörperphysik, Universität Bremen, P.O. Box 330 440, D-28334 Bremen, Germany.

†Present address: Physics Department, Williams College, Williamstown, Massachusetts 01267.

‡Present address: Department of Physics, University of California–San Diego, La Jolla, California 92093-0319.

¹B. Fluegel *et al.*, Phys. Rev. Lett. **59**, 2588 (1987).

²J. P. Sokoloff *et al.*, Phys. Rev. B **38**, 7615 (1988).

³M. Lindberg and S. W. Koch, Phys. Rev. B **38**, 7607 (1988).

⁴H. Giessen, M. Vollmer, W. Stolz, and W. W. Rühle, in *Quantum Electronics and Laser Science Conference, OSA Technical Digest* (Optical Society of America, Washington D.C., 1999), p. 58.

⁵P. Kner *et al.*, Phys. Rev. Lett. **78**, 1319 (1997).

⁶P. Kner, W. Schäfer, R. Lövenich, and D. S. Chemla, Phys. Rev. Lett. **81**, 5386 (1998).

⁷P. Kner *et al.*, Phys. Rev. B **60**, 4731 (1999).

⁸G. Bartels *et al.*, Phys. Rev. Lett. **81**, 5880 (1998).

⁹B. Haase *et al.*, Phys. Rev. B **59**, R7805 (1999).

¹⁰C. Sieh *et al.*, Phys. Rev. Lett. **82**, 3112 (1999).

¹¹U. Neukirch *et al.*, Phys. Rev. Lett. **84**, 2215 (2000).

¹²D. S. Chemla, in *Nonlinear Optics in Semiconductors I, Semiconductors and Semimetals, Vol. 58*, edited by R. K. Willardson, E. R. Weber, E. Garmiere, and A. Kost (Academic Press, Chestnut Hill, MA, 1998), p. 175.

¹³V. M. Axt and S. Mukamel, Rev. Mod. Phys. **70**, 145 (1998).

¹⁴H. J. Carmichael, L. Tian, W. Ren, and P. Alsing, in *Cavity Quantum Electrodynamics*, edited by P. R. Berman (Academic Press, Boston, MA, 1994), p. 381.

¹⁵W. Schäfer *et al.*, Phys. Rev. B **53**, 16 429 (1996).

¹⁶T. Östreich, K. Schönhammer, and L. J. Sham, Phys. Rev. B **58**, 12 920 (1998).

¹⁷V. M. Axt, K. Victor, and A. Stahl, Phys. Rev. B **53**, 7244 (1996).

¹⁸T. Meier and S. W. Koch, Phys. Rev. B **59**, 13 202 (1999).

¹⁹K. Leo *et al.*, Phys. Rev. Lett. **65**, 1340 (1990).

²⁰M. Wegener, D. S. Chemla, S. Schmitt-Rink, and W. Schäfer, Phys. Rev. A **42**, 5675 (1990).